BERKELEY ARCHAEOLOGICAL XRF LAB

Department of Anthropology
232 Kroeber Hall
University of California
Berkeley, CA 94720-3710

AN X-RAY FLUORESCENCE ANALYSIS OF MAJOR, MINOR, AND TRACE ELEMENT COMPOSITION OF ANDESITE AND DACITE SOURCE ROCKS FROM NORTHERN NEW MEXICO

by

M. Steven Shackley
Professor Emeritus and Director
Geoarchaeological XRF Laboratory
University of California, Berkeley

Report Prepared for

Dr. Robert Dello-Russo
Office of Archaeological Studies
Museum of New Mexico, Santa Fe

3 February 2012

INTRODUCTION

The analysis here of 15 volcanic rock samples from La Junta and the Oatman Quarry in the Taos Plateau Volcanic Field indicates very different major and trace element chemistry between the two groups. The Oatman rock samples are a relatively high alkali/silica andesite near dacite in composition, and the La Junta samples are a high alkali dacite similar to other dacites on the Taos Plateau (Lipman and Mehnert 1979; Newman and Nielsen 1987; Seaman 1983; Shackley 2011). The La Junta samples are nearly identical to the major and trace element composition of the Newman Dome located across the Rio Grande gorge, as reported in Shackley (2011), and are likely magmatically related.

LABORATORY SAMPLING, ANALYSIS AND INSTRUMENTATION

All archaeological samples are analyzed whole. The results presented here are quantitative in that they are derived from "filtered" intensity values ratioed to the appropriate x-ray continuum regions through a least squares fitting formula rather than plotting the proportions of the net intensities in a ternary system (McCarthy and Schamber 1981; Schamber 1977). Or more essentially, these data through the analysis of international rock standards, allow for inter-instrument comparison with a predictable degree of certainty (Hampel 1984).

All analyses for this study were conducted on a ThermoScientific *Quant'X* EDXRF spectrometer, located in the Department of Anthropology, University of California, Berkeley. It is equipped with a thermoelectrically Peltier cooled solid-state Si(Li) X-ray detector, with a 50 kV, 50 W, ultra-high-flux end window bremsstrahlung, Rh target X-ray tube and a 76 µm (3 mil) beryllium (Be) window (air cooled), that runs on a power supply operating 4-50 kV/0.02-1.0 mA at 0.02 increments. The spectrometer is equipped with a 200 l min^{-1} Edwards vacuum pump, allowing for the analysis of lower-atomic-weight elements between sodium (Na) and titanium

(Ti). Data acquisition is accomplished with a pulse processor and an analogue-to-digital converter. Elemental composition is identified with digital filter background removal, least squares empirical peak deconvolution, gross peak intensities and net peak intensities above background.

Trace Element Analysis

The analysis for mid Zb condition elements Ti-Nb, Pb, Th, the x-ray tube is operated at 30 kV, using a 0.05 mm (medium) Pd primary beam filter in an air path at 200 seconds livetime to generate x-ray intensity Ka-line data for elements titanium (Ti), manganese (Mn), iron (as $Fe_2O_3^T$), cobalt (Co), nickel (Ni), copper, (Cu), zinc, (Zn), gallium (Ga), rubidium (Rb), strontium (Sr), yttrium (Y), zirconium (Zr), niobium (Nb), lead (Pb), and thorium (Th). Not all these elements are reported since their values in many volcanic rocks are very low. Trace element intensities were converted to concentration estimates by employing a least-squares calibration line ratioed to the Compton scatter established for each element from the analysis of international rock standards certified by the National Institute of Standards and Technology (NIST), the US. Geological Survey (USGS), Canadian Centre for Mineral and Energy Technology, and the Centre de Recherches Pétrographiques et Géochimiques in France (Govindaraju 1994). Line fitting is linear (XML) for all elements but Fe where a derivative fitting is used to improve the fit for iron and thus for all the other elements. When barium (Ba) is analyzed in the High Zb condition, the Rh tube is operated at 50 kV and 1.0 mA, ratioed to the bremsstrahlung region (see Davis et al. 2011). Specific standards used for the best fit regression calibration for elements Ti- Nb, Pb, Th, and Ba, include G-2 (basalt), AGV-2 (andesite), GSP-1 (granodiorite), SY-2 (syenite), BHVO-2 (hawaiite), STM-1 (syenite), QLO-1 (quartz latite), RGM-1 (obsidian), W-2 (diabase), BIR-1 (basalt), SDC-1 (mica schist), TLM-1 (tonalite), SCO-1 (shale), all US Geological Survey standards, BR-1 (basalt) from the Centre de Recherches

Pétrographiques et Géochimiques in France, and JR-1 and JR-2 (obsidian) from the Geological Survey of Japan (Govindaraju 1994).

Major Oxide Analysis

The major oxides were acquired to determine the volcanic rock classification, according to the alkali/silica plot. This is a non-destructive analysis based on a theoretical fundamental parameter method, and as non-destructive it is not necessarily as accurate as destructive XRF analyses (see Lundblad et. al. 2011; Shackley 2011). This analysis was conducted identically to the northern New Mexico dacite study reported in Shackley (2011).

Analysis of the major oxides of Si, Al, Ca, Fe, K, Mg, Mn, Na, and Ti is performed under the multiple conditions elucidated below. This is a fundamental parameter analysis (theoretical with standards). The method is run under conditions commensurate with the elements of interest and calibrated with four USGS standards (RGM-1, rhyolite; AGV-2, andesite; BHVO-1, hawaiite; BIR-1, basalt), and one Japanese Geological Survey rhyolite standard (JR-1). See Lundblad et al. (2011) for another set of conditions and methods for oxide analyses.

CONDITIONS OF FUNDAMENTAL PARAMETER ANALYSIS[1]

Low Za (Na, Mg, Al, Si, P)

Voltage	6 kV	Current	Auto[2]
Livetime	100 seconds	Counts Limit	0
Filter	No Filter	Atmosphere	Vacuum
Maximum Energy	10 keV	Count Rate	Low

Mid Zb (K, Ca, Ti, V, Cr, Mn, Fe)

Voltage	32 kV	Current	Auto
Livetime	100 seconds	Counts Limit	0
Filter	Pd (0.06 mm)	Atmosphere	Vacuum
Maximum Energy	40 keV	Count Rate	Medium

High Zb (Sn, Sb, Ba, Ag, Cd)

Voltage	50 kV	Current	Auto
Livetime	100 seconds	Counts Limit	0
Filter	Cu (0.559 mm)	Atmosphere	Vacuum
Maximum Energy	40 keV	Count Rate	High

Low Zb (S, Cl, K, Ca)

Voltage	8 kV	Current	Auto
Livetime	100 seconds	Counts Limit	0
Filter	Cellulose (0.06 mm)	Atmosphere	Vacuum
Maximum Energy	10 keV	Count Rate	Low

[1] Multiple conditions designed to ameliorate peak overlap identified with digital filter background removal, least squares empirical peak deconvolution, gross peak intensities and net peak intensities above background.

[2] Current is set automatically based on the mass absorption coefficient.

The data from the WinTrace software were translated directly into Excel for Windows software for manipulation and on into SPSS for Windows for statistical analyses when necessary. In order to evaluate these quantitative determinations, machine data were compared to measurements of known standards during each run. AGV-1 or AGV-2, a USGS andesite standard is analyzed during each sample run for obsidian artifacts to check machine calibration (Tables 1 and 2).

DISCUSSION

The major and trace element analysis of the source rocks appears to follow the composition of andesite and dacite rocks in the Taos Plateau Volcanic Field (Boyer 2010; Eppler 1976; Lipman and Mehnert 1979; Newman and Nielsen 1987; Seaman 1983; Shackley 2011; Tables 1-4, and Figures 1-6 here). Many of the intermediate shield volcanoes on the plateau are andesite or dacite (Shackley 2011: Fig. 1). Cerro Montoso, just northwest of La Junta, and Guadalupe Mountain are good examples. If the magma source sampled somewhat more crust during emplacement, dacite, or in the case of No Agua Peak, rhyolite, was formed. These siliceous volcanics have been known to have been used for stone tool production for many years (Boyer 2010; Bryan and Butler 1940; Newman and Nielsen 1979; Seaman 1983; Shackley 2011; see also Dello-Russo 2004). These two rocks here are very similar in major oxide composition, just on either side of the andesite/dacite line (Figure 5). The Oatman Quarry rock is elementally distinctive from all other dacite sources in publication (Shackley 2011; Tables 1 and 2 here). The La Junta rock is another story.

La Junta and the Newman Dome

In 1987 Jay Newman reported a number of "rhyodacite" sources in the field. One, that was not named was a relatively small dome just east of Cerro Montoso, and just (northeast) across the Rio Grande gorge from La Junta, named the "Newman Dome" by Shackley (2011). Not surprisingly, the major oxide and trace element composition of La Junta and the Newman Dome is very similar on nearly all elements, and one sample of La Junta (sample 4) plots at nearly the same position on the alkali/silica plot (Tables 1-4, Figures 2-6). A cluster analysis based on five elements indicates close grouping of these two groups (Figure 4). It is quite possible that the La Junta samples are derived from the Newman Dome or certainly derived from the same magma source. Additionally, the alkali-silica classification indicates that the Newman Dome and the La Junta material are essentially the same (Figure 6).

SUMMARY

The analysis of these two rock sources, La Junta, and the Oatman Quarry, adds more clarity to the corpus of intermediate to silicic prehistoric stone raw material on the Taos Plateau. As others have noted, these volcanic rocks have been used as raw material from the Paleoindian through the historic periods (Boyer 2010; Bryan and Butler 1940; Newman and Nielsen 1987; Shackley 2011; Vierra et al. 2005).

REFERENCES CITED

Boyer, J.L., 2010, Identifying volcanic material sources in the Taos Valley. In Brown, E.J., Armstrong, K, Brugge, D.M., and Condie, C.J. (Eds.), *Threads, Tints, and Edification: Papers in Honor of Glenna Dean*, pp. 21-32. Papers of the Archaeological Society of New Mexico 36, Albuquerque.

Bryan, K., and Butler, A.P., Jr., 1940, Artifacts made of the glassy andesite of San Antonio Mountain, Rio Arriba County, New Mexico. University of New Mexico Bulletin Anthropology Series 3, 27-31.

Davis, K.D., T.L. Jackson, M.S. Shackley, T. Teague, and J.H. Hampel, 2011, Factors affecting the energy-dispersive x-ray fluorescence (EDXRF) analysis of archaeological obsidian. In M.S. Shackley (Ed.) *X-Ray Flourescence Spectrometry (XRF) in Geoarchaeology*, pp. 45-64. Springer, New York.

Dello-Russo, R.D., 2004, Geochemical comparisons of silicified rhyolite from two prehistoric quarries and 11 prehistoric projectile points, Socorro County, New Mexico, U.S.A. *Geoarchaeology* 19, 237-264.

Eppler, D., 1976, The Geology of the San Antonio Mountain Area, Tres Piedras, Taos and Rio Arriba Counties, New Mexico. Unpublished M.S. thesis, University of New Mexico, Albuquerque.

Govindaraju, K.1994, 1994 Compilation of working values and sample description for 383 geostandards. *Geostandards Newsletter* 18 (special issue).

Hampel, Joachim H., 1984, Technical considerations in x-ray fluorescence analysis of obsidian. In *Obsidian Studies in the Great Basin*, edited by R.E. Hughes, pp. 21-25. Contributions of the University of California Archaeological Research Facility 45. Berkeley.

Hildreth, W.1981, Gradients in silicic magma chambers: implications for lithospheric magmatism. *Journal of Geophysical Research* 86:10153-10192.

Hughes, Richard E., and Robert L. Smith 1993, Archaeology, geology, and geochemistry in obsidian provenance studies. *In Scale on Archaeological and Geoscientific Perspectives*, edited by J.K. Stein and A.R. Linse, pp. 79-91. Geological Society of America Special Paper 283.

Lipman, P.W., and Mehnert, H.H., 1979, The Taos Plateau Volcanic Field, northern Rio Grande Rift, New Mexico. In Riecker, R.E. (Ed.), Rio Grande Rift: Tectonics and Magnetism, American Geophysical Union, Washington, DC, pp. 289-311.

Lundblad, S.P., P.R. Mills, A. Drake-Raue, and S.K. Kikiloi, 2011, Non-destructive EDXRF analyses of archaeological basalts. In M.S. Shackley (Ed.) *X-Ray Flourescence Spectrometry (XRF) in Geoarchaeology*, pp. 65-80. Springer, New York.

Mahood, Gail A., and James A. Stimac
1990 Trace-Element Partitioning in Pantellerites and Trachytes. *Geochemica et Cosmochimica Acta* 54:2257-2276.

McCarthy, J.J., and F.H. Schamber 1981, Least-squares fit with digital filter: a status report. In *Energy Dispersive X-ray Spectrometry*, edited by K.F.J. Heinrich, D.E. Newbury, R.L. Myklebust, and C.E. Fiori, pp. 273-296. National Bureau of Standards Special Publication 604, Washington, D.C.

Newman, J.R., and Nielsen, R.L., 1987, Initial notes on the x-ray fluorescence characterization of the rhyodacite sources of the Taos Plateau, New Mexico. Archaeometry 29, 262-275.

Seaman, T.J., 1983, Archaeological investigations on Guadalupe Mountain, Taos County, New Mexico. Laboratory of Anthropology Note 309. Museum of New Mexico, Santa Fe.

Seaman, T.J., and Chapman, R.C. (Eds.), 1993, Guadalupe Mountain, New Mexico: an inquiry into the archaeology of place. Office of Contract Archaeology, University of New Mexico, Albuquerque.

Schamber, F.H. 1977, A modification of the linear least-squares fitting method which provides continuum suppression. In *X-ray Fluorescence Analysis of Environmental Samples*, edited by T.G. Dzubay, pp. 241-257. Ann Arbor Science Publishers.

Shackley, M.S., 2011, Sources of archaeological dacite in northern New Mexico. *Journal of Archaeological Science* 38:1001-1007.

Vierra, B., M.S. Shackley, and M. Jodry 2005, Late Paleoindian and Early Archaic Foragers of the Northern Rio Grande. Paper presented in the Symposium, *From Paleoindian to Archaic – Views on a Transition.* The 70th Annual Meeting of the Society for American Archaeology, Salt Lake City, Utah.

Table 1. Minor and trace element concentrations for the samples and AGV-1 USGS standard. All measurements in parts per million (ppm).

Source/Sample	Ti	Mn	Fe	Rb	Sr	Y	Zr	Nb	Ba	Pb	Th
La Junta											
1A	4095	746	39796	59	213	24	88	13	584	11	3
1B	3428	685	35966	60	201	20	83	14	565	11	10
2	4212	804	41745	65	214	21	86	18	443	16	5
3	4478	849	43173	66	227	20	87	18	473	15	4
4	4405	973	41546	62	225	20	83	14	467	15	4
5	4827	896	47804	68	238	22	85	14	478	9	6
Oatman Quarry											
B6	4007	611	34874	45	777	19	220	27	1544	11	3
1	4091	634	34604	42	758	16	218	22	1725	13	3
2	4271	594	34277	45	753	20	218	21	1352	9	7
3	4128	868	34851	47	764	18	220	24	1689	40	7
4	4258	624	35827	45	778	17	222	24	1563	12	4
5	4287	647	36923	46	801	19	223	21	1475	8	3
7	4284	646	35389	43	773	22	221	26	1696	9	8
9	4508	693	37859	46	786	19	223	15	1711	12	11
10	4247	659	35542	47	795	19	221	21	1539	9	3
AGV-1	5752	715	43139	71	663	21	228	15	1456	28	3

Table 2. Major oxide values for one sample each from La Junta and Oatman Quarry. All measurements in weight percent.

Sample	SiO_2 %	Al_2O_3 %	CaO %	Fe_2O_3 %	K_2O %	MgO %	MnO %	Na_2O %	TiO_2 %
LA JUNTA-4	62.73	13.996	4.77	8.552	3.29	1.785	0.375	3.129	1.108
OATMAN-4	64.495	14.967	5.187	5.943	3.019	1.337	0.111	3.779	0.761
AGV-2	61.833	15.165	5.863	7.231	3.174	1.407	0.121	3.77	1.142

Table 3. Mean and central tendency for the La Junta concentrations in Table 1.

La Junta

	N	Minimum	Maximum	Mean	Std. Deviation
Ti	6	3428	4827	4241	471.0
Mn	6	685	973	826	103.8
Fe	6	35966	47804	41671	3897.5
Zn	6	66	80	74	5.5
Rb	6	59	68	63	3.7
Sr	6	201	238	220	13.1
Y	6	20	24	21	1.8
Zr	6	83	88	85	1.9
Nb	6	13	18	15	2.1
Ba	6	443	584	502	57.8
Pb	6	9	16	13	2.6
Th	6	3	10	5	2.6

Table 4. Mean and central tendency for the Oatman Quarry concentrations in Table 1.

Oatman

	N	Minimum	Maximum	Mean	Std. Deviation
Ti	9	4007	4508	4231	143.8
Mn	9	594	868	664	81.7
Fe	9	34277	37859	35572	1160.5
Zn	9	84	99	91	4.7
Rb	9	42	47	45	1.6
Sr	9	753	801	776	16.3
Y	9	16	22	19	1.7
Zr	9	218	223	221	2.1
Nb	9	15	27	22	3.6
Ba	9	1352	1725	1588	127.0
Pb	9	8	40	14	10.2
Th	9	3	11	6	3.0

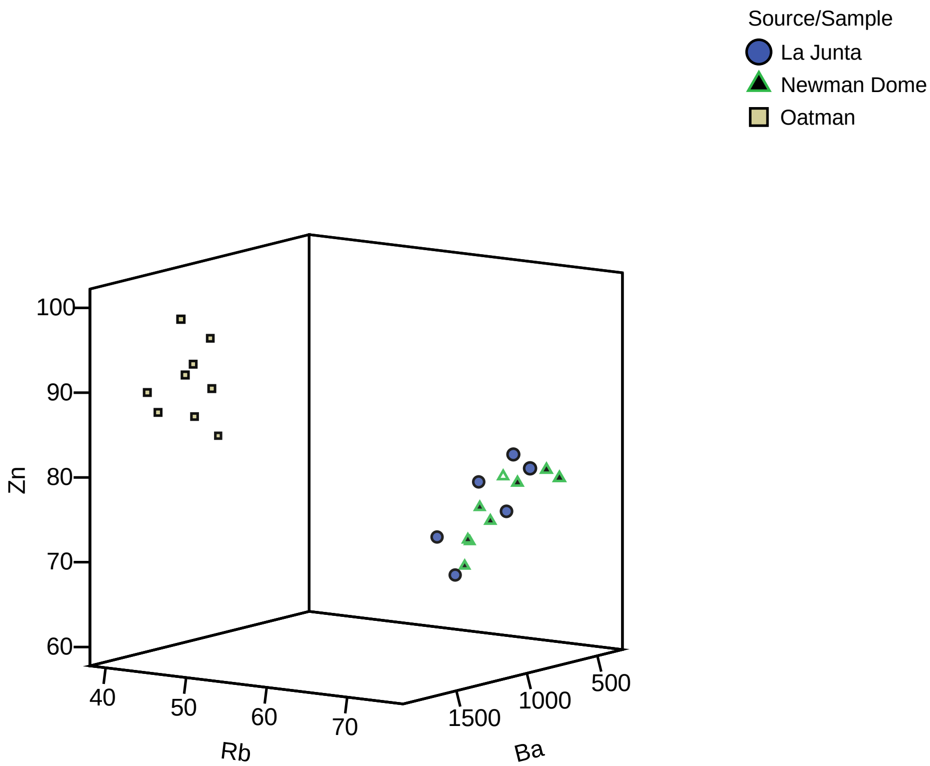

Figure 1. Rb, Zn, Ba three-dimensional plot of the La Junta and Oatman Quarry samples.

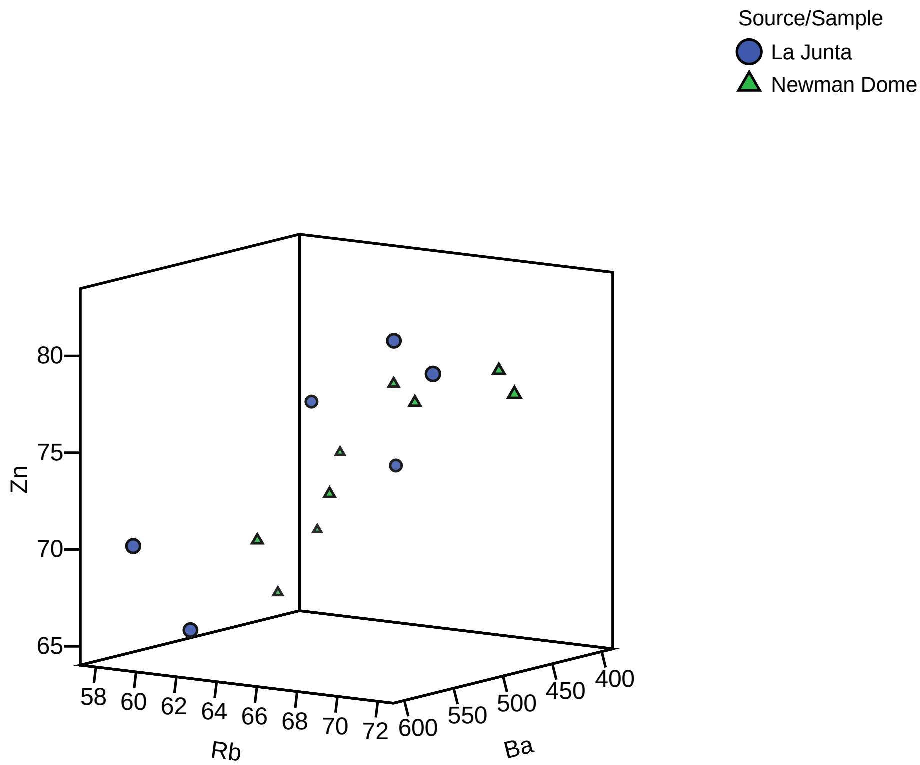

Figure 2. Rb, Zn, Ba three-dimensional plot of the La Junta and Newman Dome samples.

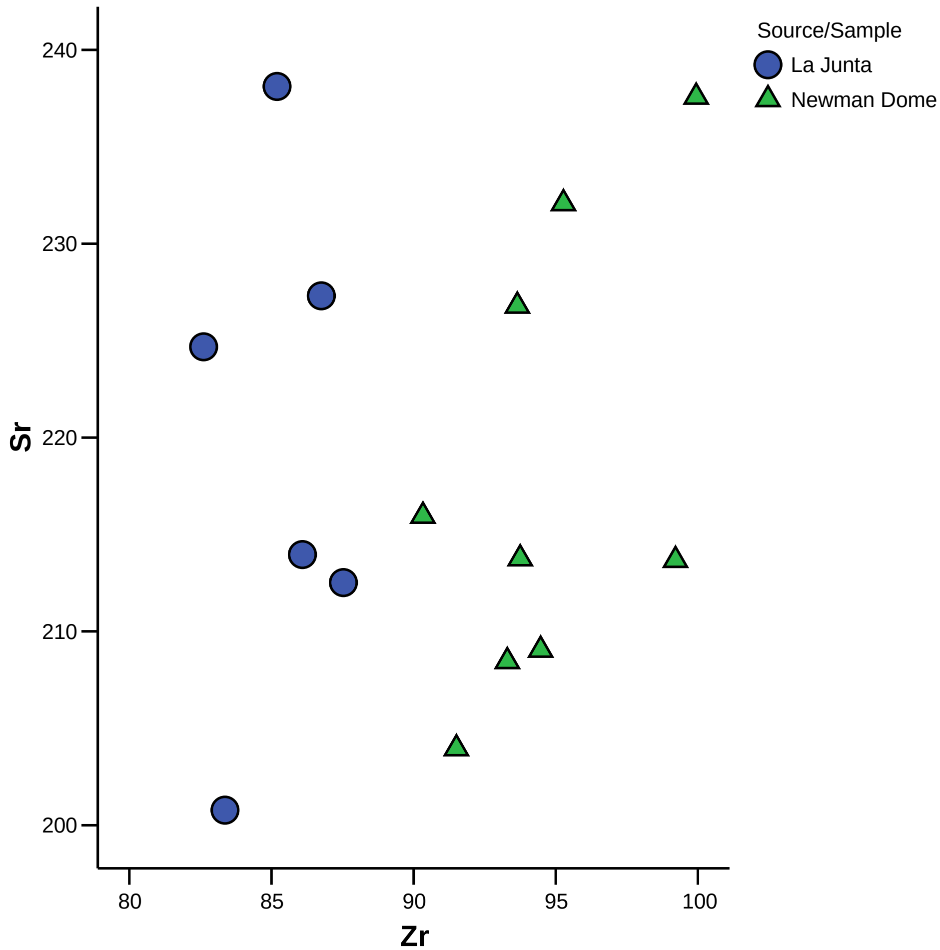

Figure 3. Zr versus Sr bivariate plot of the La Junta and Newman Dome samples. The La Junta and Newman Dome samples are slightly separated on Zr in this collection.

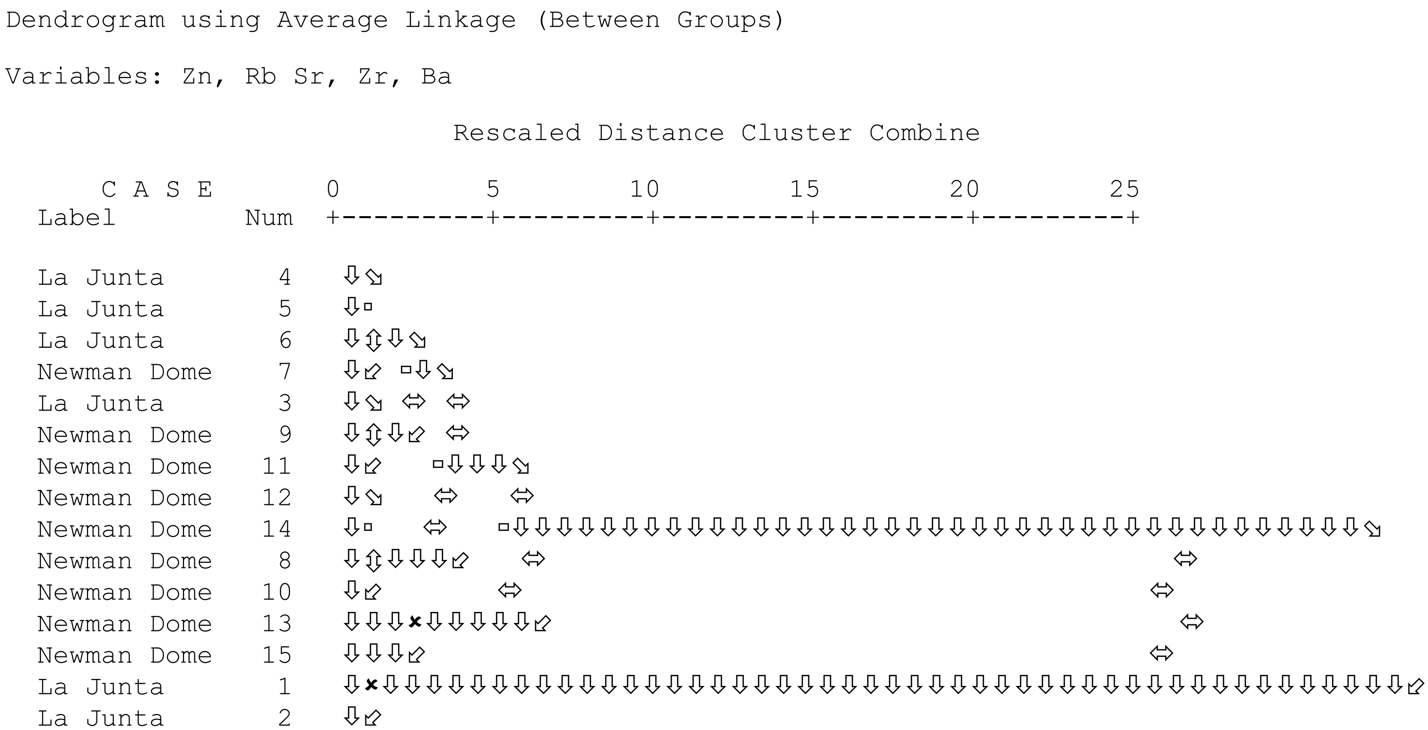

Figure 4. Hierachical cluster analysis of the La Junta and Newman Dome samples. Newman Dome samples from Shackley (2011).

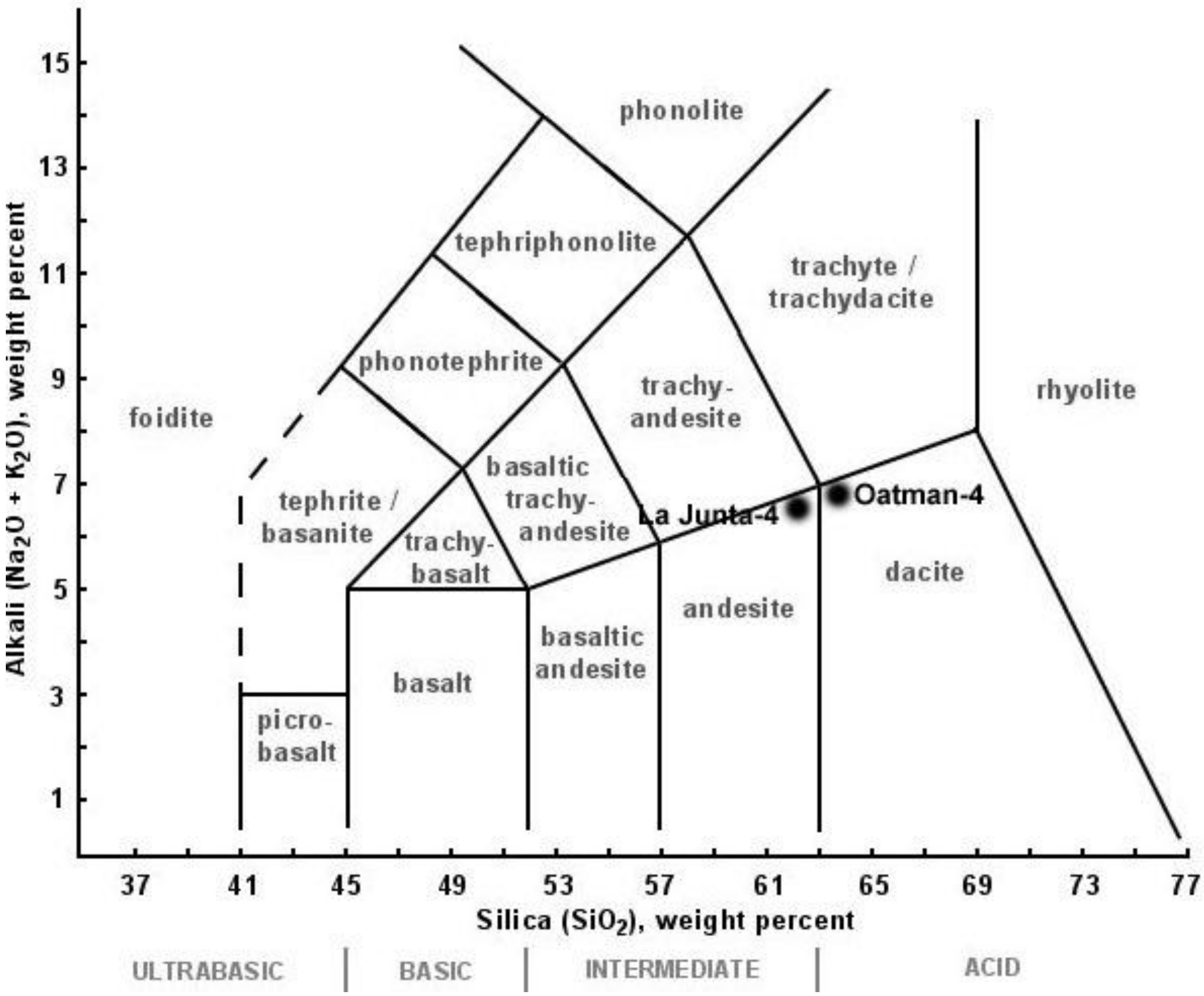

Figure 5. Alkali/silica plot of one sample of La Junta and Oatman from data in Table 2.

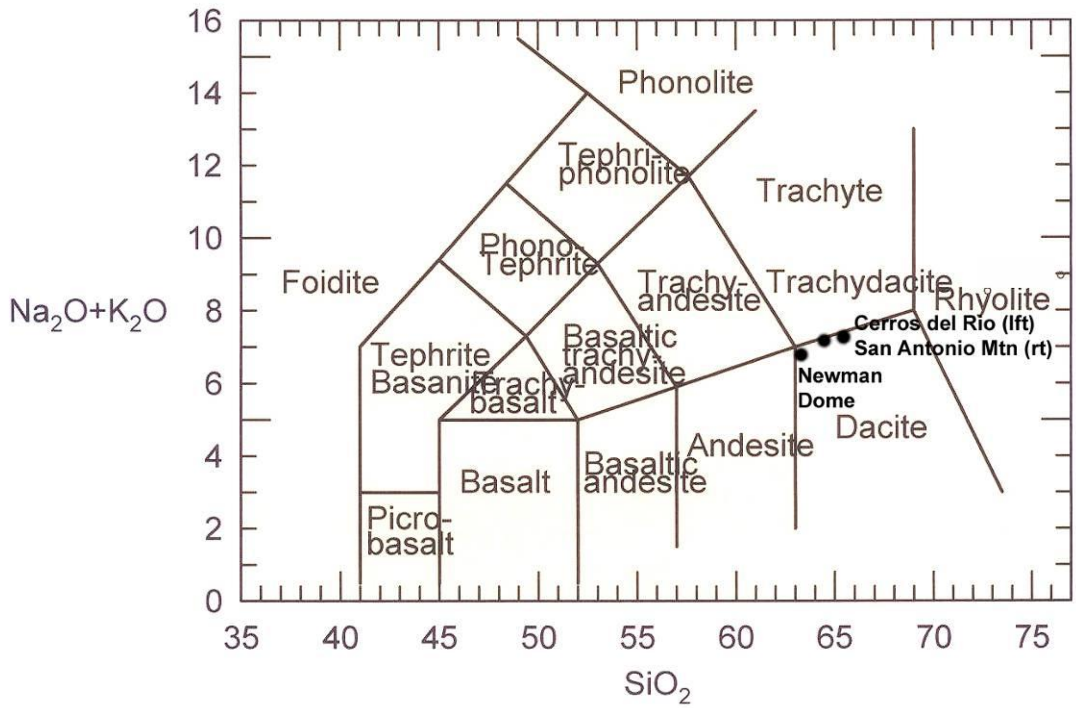

Figure 6. Alkali/silica plot of other dacite sources in northern New Mexico (from Shackley 2011). Note how similar the La Junta sample plots in Figure 5 and the Newman Dome sample in this figure.